BGSG

Volume 55

Research Paper

PROBABILISTIC SEISMIC HAZARD ASSESSMENT (PSHA) FOR LESVOS ISLAND USING THE LOGIC TREE APPROACH

Nikolaos Vavlas[1], Anastasia Kiratzi[1], Basil Margaris[2], George Karakaisis[1]

[1] Department of Geophysics, Aristotle University of Thessaloniki, 54124 Thessaloniki, Greece, navavlas@geo.auth.gr, kiratzi@geo.auth.gr, karakais@geo.auth.gr

[2] Institute of Earthquake Engineering and Engineering Seismology, EPPO, 55102 Thessaloniki, Greece, margaris@itsak.gr

Correspondence to:
N. Vavlas
navavlas@geo.auth.gr

DOI number:
http://dx.doi.org/10.12681/bgsg.20705

Keywords:
PSHA, Lesvos, earthquake, logic tree, seismic hazard

Citation:
Vavlas, N, A. Kiratzi, B. Margaris, G. Karakaisis (2019), Probabilistic seismic hazard assessment (PSHA) for Lesvos island using the logic tree approach, Bulletin Geological Society of Greece, v.55, 109-136.

Publication History:
Received: 29/06/2019
Accepted: 16/10/2019
Accepted article online: 18/10/2019

The Editor wishes to thank two anonymous reviewers for their work with the scientific reviewing of the manuscript and Ms Emmanouela Konstantakopoulou for editorial assistance.

Abstract

We carry out a probabilistic seismic hazard assessment (PSHA) for Lesvos Island, in the northeastern Aegean Sea. Being the most populated island in the northern Aegean Sea and hosting the capital of the prefecture, its seismic potential has significant social-economic meaning. For the seismic hazard estimation, the newest version of the R-CRISIS module, which has high efficiency and flexibility in model selection, is used. We incorporate into the calculations eight (8) ground motion prediction equations (GMPEs). The measures used are peak ground acceleration, (PGA), peak ground velocity, (PGV), and spectral acceleration, (SA), at T=0.2 sec representative of the building stock. We calculate hazard curves for selected sites on the island, sampling the southern and northern parts: Mytilene, the capital, the village of Vrisa, Mithymna and Sigri. Hazard maps are also presented in terms of all three intensity measures, for a mean return period of 475 years (or 10% probability of exceedance in 50 years), assuming a Poisson process. Our results are comparable to the predictions of on-going EU hazard models, but higher than the provisions of the Greek Seismic Code. Finally, we perform disaggregation of hazard to depict the relative contribution of different earthquake sources and magnitudes to the results.

Keywords: *PSHA, Lesvos, earthquake, logic tree, seismic hazard*

Περίληψη

Πραγματοποιήσαμε μια πιθανολογική εκτίμηση της σεισμικής επικινδυνότητας (ΠΕΣΕ) για το νησί της Λέσβου. Όντας το νησί του Βορείου Αιγαίου Πελάγους με το μεγαλύτερο πληθυσμό και φιλοξενώντας την πρωτεύουσα του νομού, το σεισμικό του δυναμικό έχει

μεγάλη κοινωνικοοικονομική σημασία. Η νεώτερη έκδοση του λογισμικού R-CRISIS χρησιμοποιείται για την εκτίμηση της σεισμικής επικινδυνότητας. Ενσωματώνουμε οκτώ (8) εμπειρικές σχέσεις πρόβλεψης της ισχυρής σεισμικής κίνησης (GMPEs) στους υπολογισμούς. Οι παράμετροι που χρησιμοποιούμε είναι η μέγιστη εδαφική επιτάχυνση (PGA), η μέγιστη εδαφική ταχύτητα (PGV) και η φασματική επιτάχυνση (SA), για T = 0.2 sec. Υπολογίζουμε καμπύλες σεισμικής επικινδυνότητας για επιλεγμένες θέσεις στο νησί: τη Μυτιλήνη, την πρωτεύουσα του νησιού, το χωριό της Βρίσας, πλησίον της νοτιοανατολικής ακτής, τη Μήθυμνα και το Σίγρι, στο δυτικό και νότιο τμήμα του νησιού, αντίστοιχα. Χάρτες σεισμικής επικινδυνότητας υπολογίζονται για τις τρεις παραμέτρους σεισμικής επικινδυνότητας, για μέση περίοδο επανάληψης 475 έτη (ή 10% πιθανότητα υπέρβασης στα 50 έτη), θεωρώντας κατανομή Poisson. Τα αποτελέσματά μας είναι συγκρίσιμα με αυτά πρόσφατων Ευρωπαϊκών προγραμμάτων, όμως η δική μας πιθανολογική εκτίμηση οδηγεί σε μεγαλύτερες τιμές σε σχέση με τις προβλέψεις του Ελληνικού Αντισεισμικού Κανονισμού (ΕΑΚ). Τέλος, τα αποτελέσματα απο-αθροίζονται ώστε να απεικονιστεί η σχετική συνεισφορά των διαφόρων σεισμικών πηγών και μεγεθών στα τελικά αποτελέσματα.

Λέξεις κλειδιά: *ΠΕΣΕ, Λέσβος, λογικό δένδρο, σεισμική επικινδυνότητα*

1. INTRODUCTION

Lesvos Island is located in the northeastern Aegean Sea in a transtensional tectonic setting (Fig. 1), where the deformation is taken up by both normal and strike-slip faulting revealed by seismic (Taymaz et al., 1991; Kiratzi, 2018; Papadimitriou et al., 2018) and geodetic studies (Reilinger et al., 1997; Kahle et al., 1998). The instrumentally recorded events are distributed mainly offshore, however fault activation on the island itself is clearly depicted by historical (pre-1911 for Greece) seismicity (red asterisks in Fig. 1).

The most prominent tectonic feature onshore Lesvos Island is the Agia Paraskevi Fault Zone (APFZ), a right lateral strike-slip fault (Chatzipetros et al., 2013), that runs through its central part and the Edremit Fault Zone (EFZ), a normal fault bounding the northern shoreline of the homonymous trough (Fig. 1). The APF is associated with the occurrence of the 7 March 1867 M=7.0 earthquake, which destroyed the capital and other villages of Lesvos and caused 550 deaths. The EFZ was the source of the 6 October 1944 M=6.9 earthquake, which caused severe damage mainly at Ayvacik (Papazachos and Papazachou, 2003). The most recent earthquake to affect Lesvos

Island is the 12 June 2017 M=6.3 event. Its epicenter was located offshore the southeastern coast of Lesvos and the most severe damage occurred at the village of Vrisa (Kiratzi, 2018; Papadimitriou et al., 2018; Mavroulis et al., 2019).

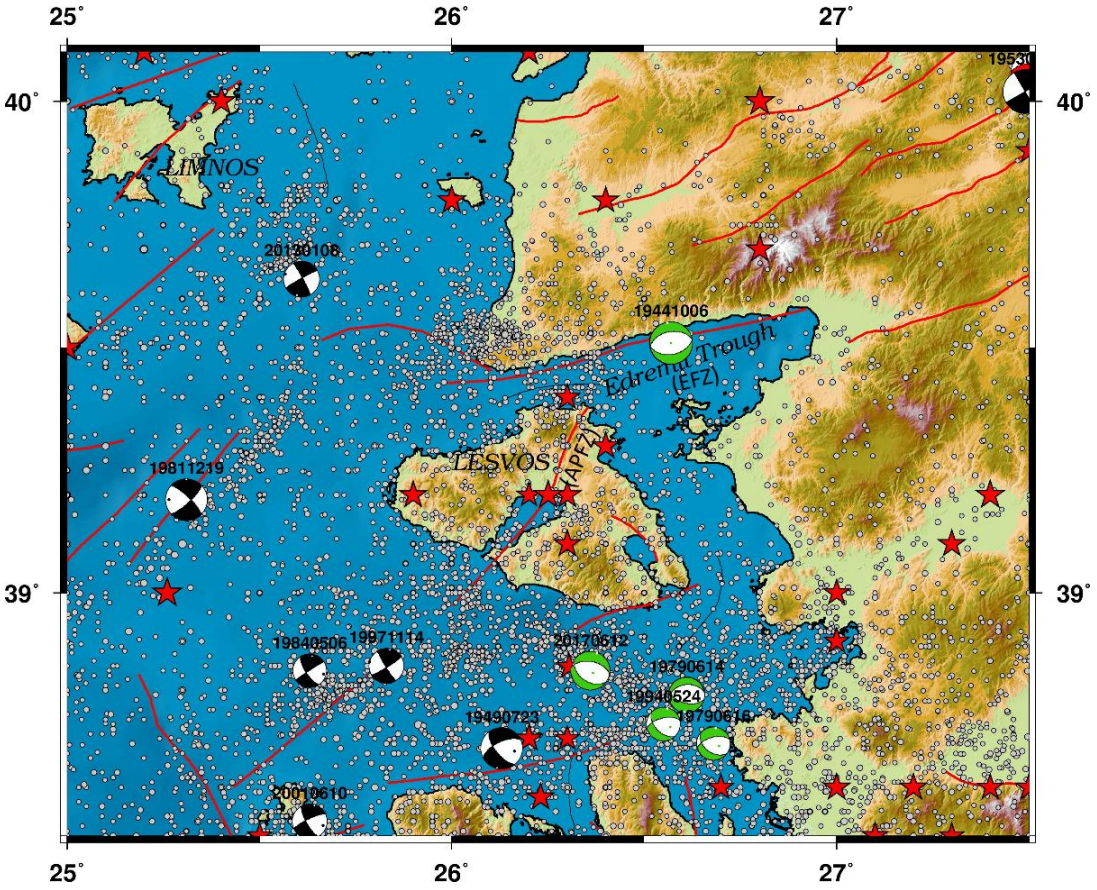

Fig. 1: Seismicity, focal mechanisms and faults of the broader region of Lesvos Island. Historical (pre-1911) earthquakes (red asterisks, Papazachos and Papazachou, 2003) and instrumental background seismicity (grey circles; on-line catalogue at http://geophysics.geo.auth.gr/ss/station_index_en.html). The focal mechanisms (beach balls) are colored black for strike-slip and green for normal faulting. The active faults (red lines) are from the European Database of Seismogenic Faults (Basili et al.2013).

Regarding the seismic hazard, according to the effective Greek Seismic Code (EAK, 2003), Lesvos belongs to Zone II of 0.24 g design acceleration for a mean return period of 475 years (or 10% probability of exceedance in 50 years). Recent EU-projects, as for example SHARE (Giardini et al., 2013, 2014) and publications (Vamvakaris et al., 2016; Tselentis and Danciu, 2010; Weatherill and Burton, 2010) indicate higher accelerations, compared to those of the Greek Code. The scope of the present work is to revisit the calculation of the seismic hazard of Lesvos, using updated seismic catalogues and suitable ground motion prediction equations (GMPEs), alongside a sensitivity analysis to identify the parameters that shape the hazard levels at selected

sites. Our intention is to compare the results with the provisions of the existing national code. In doing so, we selected to stay close to the source configuration used in the existing seismic hazard map of Greece.

2. MATERIALS AND METHODS

2.1. PSHA Methodology

The seismic hazard at a specific site is usually expressed in terms of annual exceedance rates, v, of measures of ground motion (for example, of peak ground acceleration, PGA). For instance, v(a) is the number of earthquakes per year for which PGA is exceeded at a site of interest and its inverse is the mean return period in years (Ordaz and Reyes, 1999). Assuming a Poisson (i.e. memoryless) process, the probability that, a, will exceed a specified value **a***, in a given time duration, t, is given by the expression:

$$P(a > a^*) = 1 - e^{-t \cdot v\left(a^*\right)} \tag{1}$$

Using **Eq. 1** for varying levels of **a**, one can construct hazard curves which depict the probability of exceedance for the selected **a** values, during a specified time duration, **t**. One-way to estimate **v(a*)** is by counting the times for which the value **a*** has been exceeded. This is called the empirical estimation. Given that the observation time is frequently not long enough for a reliable estimation and because accelerometric data exist only for a few sites, an indirect estimation of v (a) is carried out.

For the indirect estimation of **v(a)**, the former is alternately expressed using the total probability theorem as (Cornell, 1968, 1971; Esteva, 1970; McGuire, 2004; Tselentis and Danciu, 2010):

$$v(a > a^*) = \sum_{\mathrm{i}=1}^{\mathrm{n_{sources}}} \lambda(m_{\mathrm{i}} \geq m_{min}) \int_{m_{min}}^{m_{max}} \int_{r_{min}}^{r_{max}} P(a > a^* \mid m, r)\, f_M(m)_{\mathrm{i}}\, f_R(r)_{\mathrm{i}}\, dr\, dm \tag{2}$$

where, for a seismic source, i, $\lambda(m_i \geq m_{min})$ is the annual number of earthquakes, above a certain threshold magnitude, m_{min}, selected to have engineering significance; $P(a>a^*)$ is the probability that for a given pair of magnitude, M_i and distance, R_i from the source, PGA exceeds the value a^*; $f_M(m)_i$ is the probability density function of the magnitude m, and $f_R(r)_i$ is the probability density function of distance resulting from spatial integration (subdividing the sources).

The procedure described by **Eq. 2**, sums up all possible magnitude-distance pairs associated with all potential hazardous seismic sources. This differentiates probabilistic

seismic hazard assessment (PSHA) from deterministic (DSHA); where in the conventional form of the latter, seismic hazard is expressed through a controlling earthquake (i.e. the earthquake that is expected to produce the strongest level of shaking). Nevertheless, past events can also be used sometimes as "scenario" earthquakes in DHSA.

The PSHA methodology used here follows four steps, common in similar studies (Reiter, 1990): 1) Identifying seismic sources; 2) Assigning a recurrence earthquake model to each one of them; 3) Assigning a GMPE, which converts seismicity data into strong ground motion data; 4) Calculating seismic hazard using **Eq. 2**. The steps 1 and 2, related to this study, are described in section (2.2), while step 3, in (2.3).

In the process of creating a model for the PSHA calculations, epistemic uncertainty arises (uncertainty associated with limited data knowledge). To handle this uncertainty the logic tree approach (Kulkarni et al., 1984) is often implemented. This approach allows capturing the epistemic uncertainties in different input models by employing alternative models in the hazard estimation, with weighting factors reflecting the degree of confidence in each of them (Bommer et al., 2005; Bommer and Scherbaum, 2008). This approach was used in this study regarding both source geometry and GMPEs.

2.2. Seismic Sources

As previously mentioned, the PSHA methodology requires creating a model that represents the potential hazardous seismic sources for the area of interest. These sources can be modelled as points, lines, areas, or even volumes depending on the available data, the nature of the source and the options that each software offers. In our calculations, we used the latest version of R-CRISIS (Ordaz et al., 2017; Ordaz and Salgado-Gálvez, 2017) which offers all the aforementioned options. Applications with earlier versions of the CRISIS code include the work of Stylianou et al., (2016) who examined the seismic hazard of North Aegean Trough and the surrounding lands. Here, we use the additional tools and options of the new R-CRISIS module, not yet fully utilized. We only focus on shallow events, because these are more hazardous to the island, also taking into account that the island is at a long distance from the location of the intermediate-depth earthquakes, along the Hellenic Subduction Zone.

We considered two seismic source models in our calculations (**Fig. 2**): a) the faults proposed by Papazachos et al., (2001) (hereafter cited as PPZ01) and b) the seismic zones proposed by Papaioannou and Papazachos (2000) [PP00]. For the scope of the

present work, we chose this configuration, even though new data are available, (Giardini et al., 2013; Basili et al, 2013), because it was the one adopted in the Greek Seismic Code. However, we do employ newly developed ground motion prediction equations.

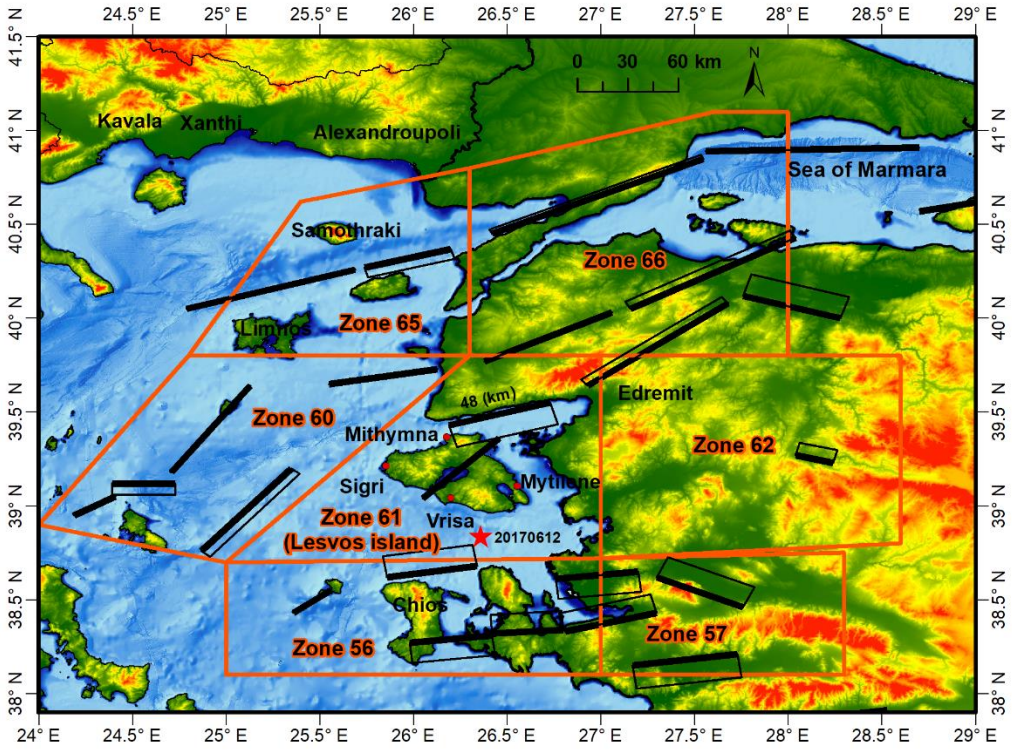

Fig. 2: Seismic sources employed into the logic tree calculations. The orange polygons indicate the zones of Papaioannou and Papazachos (2000). Black polygons denote the fault sources as in Papazachos et al. (2001) and the bold black lines depict the trace of the upper edge of each fault plane. We calculate the seismic hazard at four sites (red dots) on Lesvos Island (Sigri, Vrisa, Mytilene and Mithymna).

Concerning the PP00 model, we employed into the calculations the zones: 56, 57, 60, 61, 62, 65 and 66, while regarding the PPZ01 model, the faults that are within or partially within these zones. As will be shown later, from the hazard disaggregation, these geographical limits, are more than enough for the hazard estimation for the four sites of interest, as more than 95% of the total probability of exceedance (for all magnitudes and for a mean return period of 475 years) is contained in the 0-60 km source to site distance range. No historical or instrumental event beyond these geographical limits has ever caused significant damage to the Island of Lesvos (Papazachos and Papazachou, 2003). The employed seismic sources are shown in **Fig.**

2 where the orange polygons indicate the zones used and the black bold lines represent the traces of the faults plane's upper edges.

A minimum magnitude, m_{min}, equal to **M** 5.0 was used in both source models. There are several_reasons for this choice. Firstly, as discussed by Bommer and Crowley (2017), m_{min}, is an engineering rather than a seismological parameter and its choice is related to seismic risk and not seismic hazard. In addition, the majority of ground motion prediction equations (GMPEs) proposed for the Greek region have a lower bound of applicability ~ at **M** 5.0. The extrapolation of GMPEs should be avoided and it is questionable whether they should be used at the limits of their applicability range (Bommer et al., 2007). Finally, examining how sensitive the calculations are to the choice of m_{min} (**Fig. 4**), the differences found were insignificant.

Regarding the PP00 model (orange polygons, **Fig. 2**), we used the fault plane solutions assigned to every seismogenic source by Moratto et al. (2007). Based on the dip of the P- and T- axes, we assigned a proper coefficient accounting for the type of faulting into the GMPEs (section 2.3). The strike of faulting was used to orientate the major axis of the assumed elliptical ruptures parallel to it. Concerning the aspect ratios (rupture width/rupture length) of the ellipses, we used the ones proposed by Kiratzi et al., (1985) which are 0.5 for normal faulting and 0.25 for strike-slip faulting. The rupture area, A, in relation to magnitude, **M**, was determined from the scaling relationships of Papazachos et al. (2004) applicable to Greece, which are:

$$\begin{aligned} &\textbf{Strike Slip Faulting} \\ &\textbf{LogA (km}^2\textbf{)} = 0.82\mathbf{M} - 2.79,\ \sigma = 0.19 \\ &\textbf{Dip Slip Faulting} \\ &\textbf{LogA (km}^2\textbf{)} = 0.78\mathbf{M} - 2.56,\ \sigma = 0.21 \end{aligned} \qquad (3)$$

The sources were also treated as leaky boundaries, meaning that the ruptures were allowed to extend beyond the source boundaries. A general uncertainty of 0.25 was used in the maximum magnitude, m_{max} (Papazachos et al., 1997). We adopted the maximum magnitudes, as listed in Papaioannou and Papazachos (2000), however, as they did not account for any uncertainty, a uniform probability distribution with a weight concentration equal to 1 at m_{max} was assigned. As for the focal depth of each zone, we followed the same approach used by Tselentis and Danciu (2010) and assigned a mean depth of 10 km to all sources.

The fault sources of the PPZ01 model (black polygons in **Fig. 2**) were modelled as rectangular faults. The *b* values assigned to them, are those proposed by Hatzidimitriou et al. (1994). The maximum magnitude of each source, as well as the fault's width, were determined from the scaling relationships of Papazachos et al. (2004), which are:

Strike Slip Faulting
LogL (km) = 0.59**M** - 2.30, $\sigma = 0.14$
LogW (km) = 0.23**M** - 0.49, $\sigma = 0.24$

(4)

Dip Slip Fauling
LogL (km) = 0.50**M** -1.86, $\sigma = 0.13$
LogW (km) = 0.28**M** - 0.70, $\sigma = 0.25$

An uncertainty in m_{max} was again used, 0.24 for normal faults and 0.26 for strike-slip faults, both values resulting from the scaling relationship's (σ) term. The sources were treated as strict boundaries, meaning that rupture areas were not allowed to extend outside the limits defined by the geometry of each source. For the rupture area, the relationships from **Eq. 3** were used. A minimum magnitude of **M** 6.0 was assigned to the fault sources and in addition, a background seismicity model (Woessner et al., 2015), for earthquakes not associated with a particular fault, with magnitudes 5.0≤**M**≤5.9 was used.

Both models were combined using a logic tree. The PPZ01 model, in which strong earthquakes (**M**≥6.0) can only occur on seismogenic faults, whereas smaller earthquakes (5.0≤**M**≤5.9) are scattered in the background seismicity zones, is more pragmatic. The PP00 model, where earthquakes with magnitudes 5.0≤**M**≤m_{max} have an equal probability to occur anywhere in the zone's surface, is less. Based on test calculations and expert judgement, a 0.7 weight was assigned to PPZ01 model and a weight of 0.3 to the PP00 model. We also explored the sensitivity of the hazard curves to the weight combination used (see **Fig. 6**).

2.3. Ground Motion Prediction Equations

After the source geometry and the seismicity associated with each individual source are adopted and in order to calculate the intensity of the ground motion, suitable GMPEs were selected. Here we used GMPEs in terms of peak ground acceleration, (PGA), peak ground velocity, (PGV), and spectral acceleration, (SA) at T=0.2 sec, which is representative of the building stock of the sites of interest. The scatter associated with the GMPEs is incorporated into the calculations through probabilistic concepts. This is

done to handle aleatory variability (variability related to an apparent randomness in nature). In general, given a magnitude and a distance, intensity, a^*, it is assumed to be a random variable with a given probability distribution (usually lognormal). The median predicted value of the GMPE is the 1st moment of the distribution, whereas the 2nd moment is the standard deviation of the natural logarithm. Through this, the term $P(a>a^*)$ from **Eq. 1** is computed by integrating the probability density function resulting from a given magnitude and distance pair, from a* to ∞.

R-CRISIS offers the option of a hybrid (or composite) attenuation model as an alternative for the logic tree approach, when the only difference between the models is the GMPE. When using the hybrid model, the seismic hazard intensity is treated as a hybrid random variable and not a lognormal one. This option offers a robust and straightforward way to incorporate GMPEs into the calculations without adding additional logic tree branches.

Thus, we decided to use the option of a hybrid attenuation model, because it yields the same results, in terms of expected values, as the logic tree approach (Thomas et al., 2010). Moreover, we adopted the default option and did not apply any truncation to the hazard intensity values. In general, in PSHA studies it is common practice to truncate the ground motion variability to a certain standard deviation, σ or intensity value. It has been shown (EPRI, 2006) that ground motion variability is consistent with a lognormal distribution up to at least 3σ (Abrahamson, 2006). In a number of our calculations using a single GMPE (see **Fig. 9**), we noticed a progressively minor increase in the exceedance probabilities when truncating to standard deviations greater than 3σ. This indicated that a truncation to 3σ would be sufficient to capture the aleatory variability. We propose further future investigation regarding the hybrid attenuation model and ground motion variability.

The choice of GMPEs is a process of great importance and not a trivial task. For our selection, we initially reviewed the R-CRISIS library, which has a plethora of built-in equations. To distinguish between suitable candidates, we used the procedure suggested by Cotton et al., (2006) combined with expert judgment while also reviewing the selections made among different experts in peer reviewed literature (Giardini et al., 2013; Giardini et al., 2014; Vamvakaris et al., 2016; Tselentis and Danciu, 2010; Weatherill and Burton, 2010). Against this background, we progressively rejected non-suitable GMPEs until we were left with equations that meet our criteria (**Fig.** 3 and **Table 1**).

Table 1 - Information on the suite of GMPEs incorporated into the calculations with their associated weights (last column, shown in parentheses). The abbreviations used in the magnitude range and the weight scheme, are: SS=Strike-Slip, NM=Normal faults, RV=Reverse faults, [BS] =Background Seismicity.

GMPEs	Code	Valid Magnitude Range	Valid Distance Range (km)	Type of Distance Metric	σ_{LN} (PGA)	Region	Weight (in parenthesis)
Abrahamson et al., (2014) (NGA-West 2)	AB14	3.0–8.5	0-300	R_{rup}	Varying	Worldwide	PGA (1.5) SA (1) PGA [BS] (1) SA [BS] (1)
Akkar and Bommer (2010)	AK10	5.0–7.6	1-100	R_{jb}	0.643	Europe and Middle East	PGA (2.5) SA (2) PGA [BS] (2) SA [BS] (1.5)
Boore et al., (2014) (NGA-West 2)	BO14	3.0–8.5 (SS) 3.0–8.5 (RV) 3.3–7.0 (NM)	0-400	R_{jb}	Varying	Worldwide	PGA (1.5) SA (1) PGA [BS] (1) SA [BS] (1)
Campbell and Bozorgnia (2014) (NGA-West 2)	CB14	3.3–8.5 (SS) 3.3–8.5 (RV) 3.3–7.0 (NM)	0-300	R_{rup}	Varying	Worldwide	PGA (1.5) SA (1) PGA [BS] (1) SA [BS] (1)
Chousianitis et al., (2018)	CH18	4.0–8.0	1-200	Epicentral	0.656	Greece	PGA (3) PGV (1) PGA [BS] (3) PGV [BS] (1)
Danciu and Tselentis (2007)	DT07	4.5–6.9	1-136	Epicentral	0.670	Greece	PGV (1) PGA [BS] (3) SA [BS] (2)
Segou and Voulgaris (2013)	SV13	4.5–6.6	0-150	Epicentral	0.818	Greece, Turkey, Iran	PGV (1) PGA [BS] (3) SA [BS] (2)
Skarlatoudis et al., (2003, 2007)	SK03	4.5–7.0	1-160	Epicentral	0.659	Greece	PGV (1) PGA [BS] (3) PGV [BS] (1)

We decided to include the GMPE of Akkar and Bommer (2010) (hereafter cited as AK10) because it was derived using data from Europe and Middle East. In addition, we included three GMPEs proposed in the NGA-West 2 database, namely the ones from Boore et al., (2014) [BO14], Abrahamson et al., (2014) [AB14] and Campbell and Bozorgnia (2014) [CB14]. The equation of Chiou and Youngs (2014) was not used because its median predicted values, as well as the results from the hazard calculations, were found almost equal with those of CB14. To decrease computational time and avoid further complexity into the logic tree input, CB14 was preferred due to the usage R_{jb} distance metric, which projects rupture area into the ground surface making focal depth a non-factor.

We later incorporated recent additional equations obtained using Greek data, namely those of Skarlatoudis et al., (2003; 2007) [SK03], Danciu and Tselentis (2007) [DT07], Segou and Voulgaris (2013) [SV13] and of Chousianitis et al., (2018) [CH18]. For the sake of completeness, it is worth mentioning pre-2003 equations, which were not used, based on our criteria. The first efforts for such empirical equations for shallow earthquakes in Greece were made by Theodulidis (1991) [TH91] and Theodulidis and Papazachos (1992) [TP92] based on strong motion data recorded in Greece and other worldwide regions with similar seismotectonic settings. A decade later Margaris et al., (2002) [MA02] derived updated equations based solely on Greek strong ground motion data. Additionally, another equation implemented in the Greek Seismic code is the one by Makropoulos and Burton (1985b) [MB85], which was derived by averaging eight models, available at that time.

It is worth mentioning that MB85, TH91 and TP92 are based on the surface-wave magnitude, Ms instead of Mw, which is nowadays the preferable magnitude scale. Even though these two magnitudes are approximately equal for the range 6.0 to 8.0 (Papazachos et al., 1997) and conversion relationships do exist, we refrained from inserting additional uncertainty in our calculations. Furthermore, MB85 does not report a sigma (σ) term and all the above-mentioned not used GMPEs do not sufficiently account for the soil characterization in comparison with the more recent equations. Considering the MA02 and SK03 equations, we determined that since they have a very similar functional form, the more recent derived SK03 equation partially superseded the former. In addition, MA02 does to account for faulting mechanism and for these reasons it was decided not to be included into the calculations.

For the suite of GMPEs selected, the variation of the median predicted values in relation to epicentral distance is shown in **Fig. 3** for a mean focal depth of 10 km, **M** 6.5, rock conditions and normal faulting. The calculation of the PGVs is not straightforward, because the built-in equations of R-CRISIS library are available only for the prediction of ground acceleration and not ground velocity. At the same time, their functional form is too complicated to manually insert and validate them into the software and outside the purpose of this study. For this reason, for the hazard estimation in regards to PGV, we used only the equations estimated using Greek data. Keep in mind that regarding PGV, extrapolation does happen during the calculations since the GMPEs incorporated have a narrow applicability range.

The weights assigned to each GMPE (**Table 1**) were based on expert judgment following the recommendations of the Senior Seismic Hazard Analysis Committee

(Budnitz et al., 1997). However, it must be noted that even with these general guidelines regarding expert judgment, a straightforward quantitative approach is not obvious in the literature up to the present time. The weights adopted for the GMPEs were based on the following criteria: a) The usage of data from Greece and adjoining regions, in the regression procedure, b) the applicability range (extrapolation was avoided). From this perspective, the more suitable equation in regards to PGA was CH18. Having this in mind, this equation was found to predict the highest median values, as well as the highest exceedance probabilities in the hazard calculations (see **Fig. 4**). Concerning SA, the highest weight was assigned to AK10, while regarding PGV, equal weights were assigned among the GMPEs obtained using Greek data.

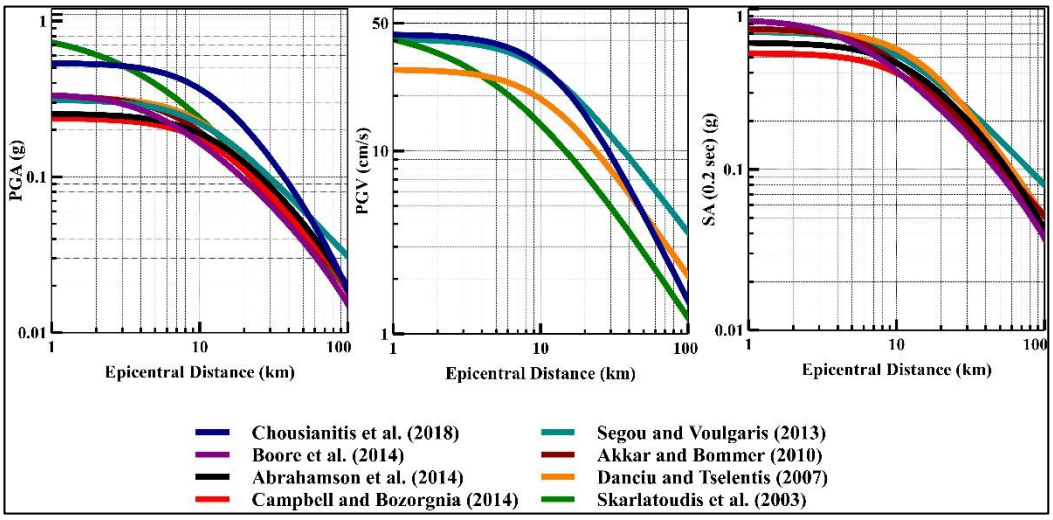

Fig. 3: Variation of the median predicted value of PGA (left) PGV (centre) and SA (at T=0.2 sec) (right) in relation to epicentral distance, for **M**=6.5, rock conditions, normal faulting and a mean focal depth of 10 km according to the GMPEs used in this study.

The relatively narrow applicability range of the GMPEs proposed for the Greek region is a limitation that needs to be considered in the hazard modelling process. For example, the SV13 equation has application in the range of **M**=4.5–**M**=6.6. The same applies for SK13 and DT07 (**Table 1)**. For this reason, the aforementioned equations were not used in the PP00 model in terms of PGA and SA, since this model covers a wide range of earthquake sizes. They were also not considered suitable for the faults of the PPZ01 model considering that m_{max} is for a number of cases beyond their upper applicability limit. Nevertheless, they were used in the background seismicity sources of the PPZ01 model, which cover earthquake magnitudes in the range of 5.0≤**M**≤5.9. On the contrary, CH18 has applicability in the range **M** 4.0–**M** 8.0 which makes it a suitable candidate for all the sources of both models.

It is also worth mentioning that the different distance definitions used among the GMPEs have a significant impact in the hazard calculations. The GMPEs proposed for the Greek region solely use epicentral distance. A number of others use, R_{jb} (Joyner and Boore, 1981), the closest distance to the projection of the fault plane on the earth's surface and R_{rup}, the distance closest to the rupture area. The R_{jb} and R_{rup} distances are arithmetically calculated for each magnitude bin through scaling relationships **Eq. 3**. Note that rupture dimensions and the depth of the sources are not taken into account when using epicentral distance, as the site to source distance is not affected in that case.

3. RESULTS

3.1. Hazard Curves

The results of the seismic hazard assessment can be represented both in terms of hazard curves for specific sites, as well as spatially, in the form of maps, by calculating a hazard curve for a grid of points and then depicting the spatial variation of the intensity corresponding to a constant mean return period. First, we present in **Fig. 4** the hazard curves in terms of PGA for the city of Mytilene, alongside the hazards curves that correspond to the Zone II (0.24 g) of the Greek Seismic Code and to the SHARE (arithmetic mean) project. The results were obtained using only the PP00 model and for each GMPE, separately. Significant variability can be observed between different GMPEs, suggesting that the calculations are sensitive to weight choice.

As we already discussed no significant variation is observed when increasing m_{min} from 4.0 to 5.0, as illustrated by the dashed curves that were obtained using the hybrid attenuation model. Note that the obtained hazard curves indicate higher exceedance probabilities in comparison with the corresponding curves from the SHARE program (Giardini et al. 2013, 2014) and the Greek Seismic Code. An important factor leading to this is the strike-slip (instead of normal) focal mechanism chosen for the zone (61) of Lesvos, which consistently increases the predicted values in GMPEs. This zone is dominated by the operation of the Agia Paraskevi Fault Zone, with a well-determined shear motion component (Chatzipetros et al., 2013). This is not the first time that higher seismic hazard levels have been calculated for Greek sites. In the framework of the SEAHELLARC project, the seismic hazard of the Pylos broader region in southern Peloponnese was examined, using the CRISIS code (SEAHELLARC Working Group, 2010). In a number of their calculations, they also used the Papaioannou and Papazachos (2000) sources and their associated seismicity combined with the TP92 GMPE. They found remarkably higher results for Pylos (0.56 g for a return period of

475 years) than those (0.143 g or 0.29 g) in the (at the time available) literature. They hypothesized that a fully probabilistic approach was not followed in the past and the aleatory uncertainty of the GMPE was not implemented in the calculations. As a test, we here used the same TP92 GMPE and we calculated the hazard curves for Mytilene with and without including the aleatory variability (**Fig.** 4). For a mean return period of 475 years we calculated a PGA = 0.52 g for σ=0 and PGA=0.93 g when incorporating the σ term. These results also imply that aleatory variability is a major factor in the calculations and the way it was handled in the past may have played a role in shaping the lower acceleration value in the Greek Seismic code.

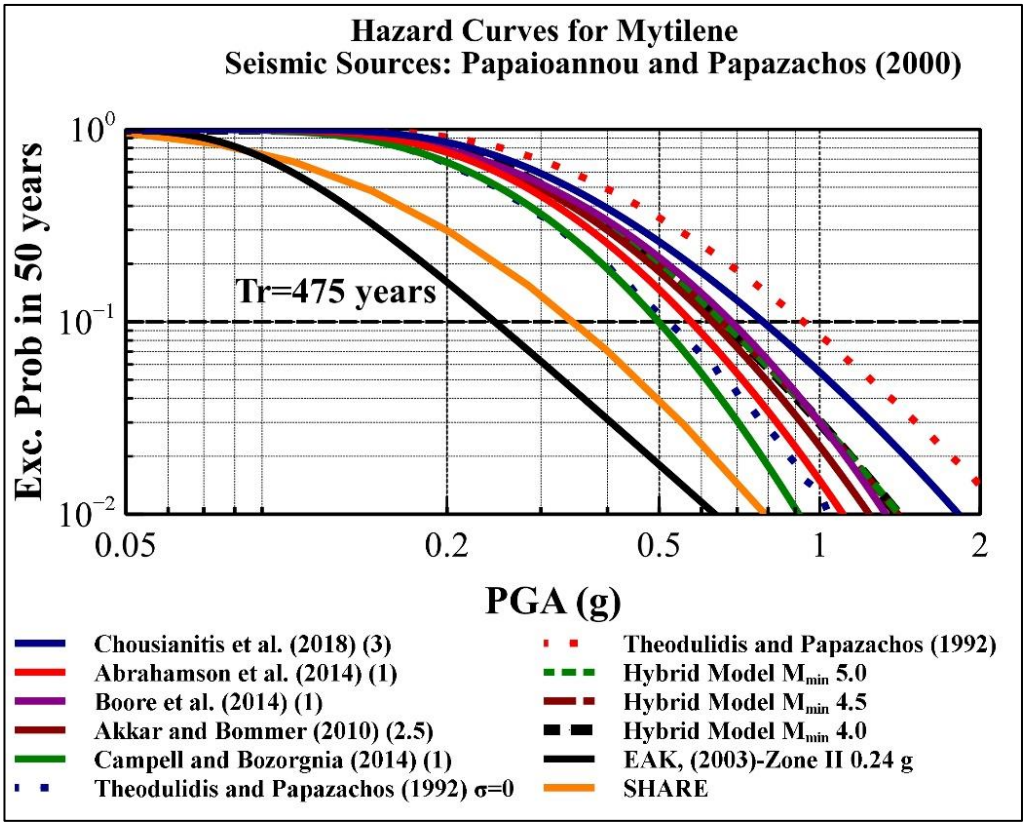

Fig. 4: Hazard Curves for Mytilene (the capital of Lesvos Island) using the PP00 model and each GMPE separately. The results using the composite (hybrid) attenuation model are shown for three different m_{min} values (dashed curves), where no significant variation is observed. The hazard curve for the Zone II (0.24 g) of the Greek Seismic Code is depicted with the black line, alongside the hazard curve (arithmetic mean) from the SHARE program (orange line). The calculations resulting using the TP92 GMPE are also presented (see text for a detailed description).

Subsequently, the PP00 and PPZ01 models were combined using the logic tree approach using a weight of 0.3 and 0.7, correspondingly. We chose four sites of interest (red dots in **Fig. 2)**: Mytilene, the capital, the village of Vrisa, close to the southeastern

coast, Mithymna and Sigri, at the northwestern and southwestern part of the island, respectively. **Fig. 5** summarizes the corresponding hazard curves along with the SHARE program results for these four examined sites (for PGA and SA) and the Zone II-0.24g (EAK, 2003) hazard curve (for PGA). We can observe that there is generally a good agreement of our results with the ones of the SHARE program, although ours appear slightly increased. The individual intensity values for a mean return period of 475 for the selected sites on the island are presented in **Table 2**. Even though there is no significant variation between the four sites according to the SHARE program results, our results indicate that Mithymna and Vrisa present slightly higher values in comparison with Sigri and Mytilene. This is due to Vrisa and Mithymna being close to the Agia Paraskevi and the Edremit fault zones, respectively. Sigri and Mytilene are located at almost equal distances from the Agia Paraskevi fault and exhibit similar seismic hazard.

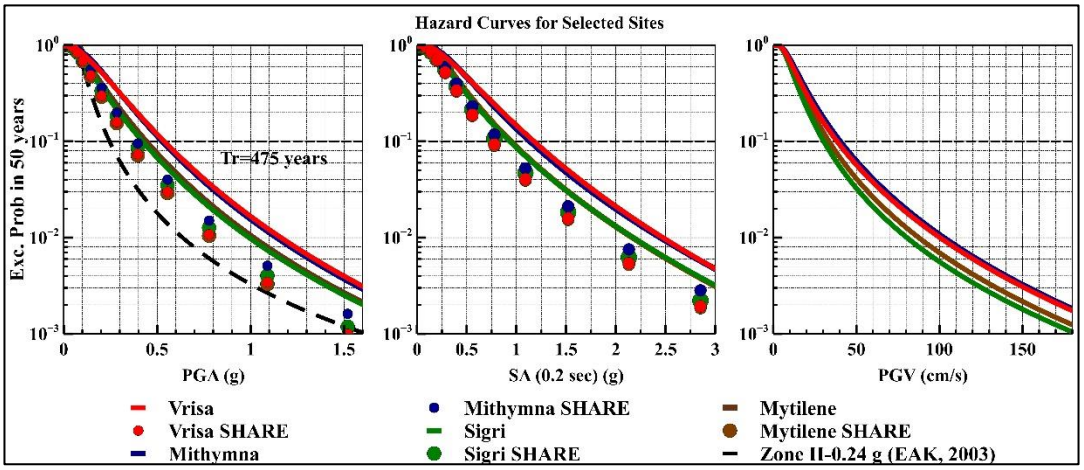

Fig. 5: Hazard Curves for the four sites of interest (red dots in Fig. 2), in terms of PGA, PGV and SA (at T=0.2 sec). The corresponding results from the SHARE program can also be seen (dots), as well as the hazard curve from the Greek Code (black dashed line) Zone II (0.24 g).

Table 2 - PSHA calculations for the four sites of interest and a mean return period of 475 years.

Mean Return Period=475 years	PGA (g)	PGV (cm/s)	SA (0.2 sec) (g)
Mytilene	0.44	34	0.94
Vrisa	0.54	38	1.18
Mithymna	0.53	40	1.14
Sigri	0.42	30	0.93

While we chose the weights of the source models based on expert judgment, it is interesting to see the effect of different weight choice combinations. This is illustrated in **Fig. 6** where it can be observed from the hazard curves of Mytilene, that the calculations are very sensitive to the weight choice. The PP00 model leads to higher seismic hazard estimation in comparison with PPZ01, thus increasing the weight in the former increases the results. In the same figure the resulting hazard curve using only the PPZ01 model branch is shown (dark red constant line), which resembles (in comparison with the rest) the curve from the Greek Seismic Code.

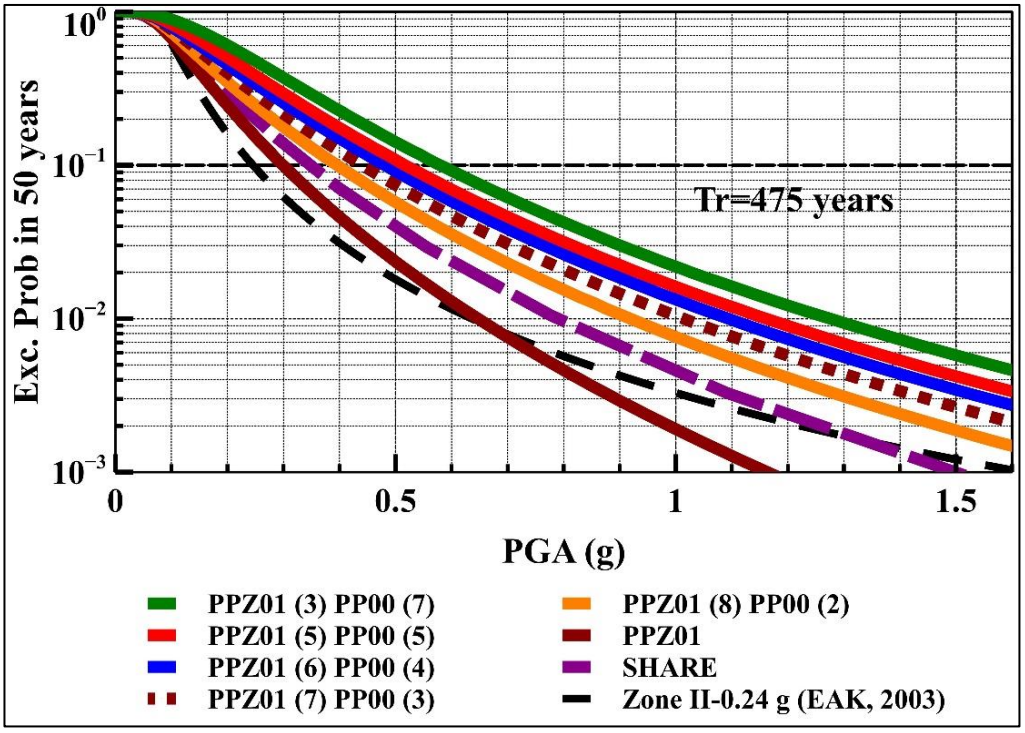

Fig. 6: Hazard Curves for the city of Mytilene resulting from different weight choice combinations. It is noticeable that the calculations are sensitive to weigh choice. The corresponding curves from the Greek Seismic code (black line) and the SHARE program (purple line) are presented. The dark red line was obtained using only the PPZ01 model.

3.2. Hazard Maps

In **Fig. 7** the hazard maps of the Lesvos Island for a mean return period of 475 years are presented. These resulted from a computation over a grid of points with origin's coordinates: longitude 25.8º and latitude 38.9º. An increment of 0.08º was used for 12 points along longitude and 8 along latitude. It is observed that, the Agia Paraskevi fault has a dominant effect in the central part of the island where PGA, SA and PGV values

are higher and as we move to the east or the west, lower values are observed. In the same figure, the calculated values for the four sites of interest are presented. Similar values are observed between Mithymna and Vrisa as well as between Mytilene and Sigri.

The effect of different distance definitions in the GMPEs is also depicted. The GMPEs that have been used in terms of PGV are the most recent ones proposed for the Greek region (**Table 1**), which use epicentral distance. In the hazard maps, referring to this intensity value, we can see the potential earthquake focus is concentrated in the central part of the island, midway of the Agia Paraskevi fault's trace, which is very steep (dip angle of 89°). This is because the faults were treated as strict boundaries and the epicentres were only allowed in this specific part of the fault. At the same time, regarding PGA and SA, the different distance definitions used among the NGA-WEST 2 and AK10 GMPEs result in equal intensity curves that have a different shape.

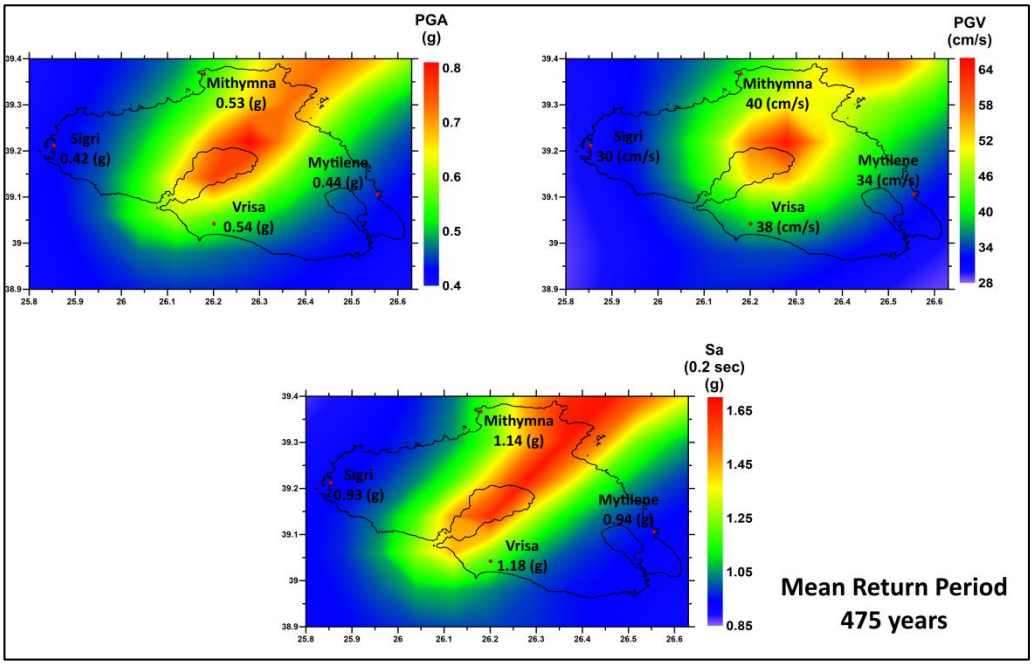

Fig. 7 Hazard maps resulting from a computation over a grid of sites. The spatial variation of the intensity value that corresponds to a constant mean return period of 475 years is presented.

3.3. Disaggregation

One of the extensions of PSHA is the hazard disaggregation (McGuire, 1995; Bazzurro and Cornell, 1999). We mentioned in section (2.1) that into the PSHA computations, all the possible magnitude and distance scenarios are aggregated into a single result. We can disaggregate all these scenarios into magnitude and distance bins and depict the

relative contribution of each one of them into the result. This is done for a single point of interest, in which a probability of exceedance in a given time period is chosen (which corresponds to a specific intensity level), or an intensity level directly. After this, the bins that correspond to this intensity level which were initially used to calculate the exceedance probability are presented into (usually) 3D diagrams. In addition, while disaggregating the results an *epsilon (ε)* value is chosen, which is the number of standard deviations from the median value. Thus, the term P ($a>a^*$) is calculated by integrating the probability density function of the GMPE from a^* to a_ε, instead of integrating from a* to ∞, where:

$$a_\varepsilon = \text{Median}\,(a \mid m,r)\cdot exp\left[\varepsilon \cdot \sigma_{ln}(a \mid m,r)\right] \quad (5)$$

In this way, the percentage of exceedance probability contained in different areas (from a^* to a_ε) of the GMPEs probability density function can be calculated. Because of the way uncertainty is being handled in the hybrid attenuation model, we decided that it is more appropriate to disaggregate the results using only the AK10 equation and the PPZ01 model. This GMPE was chosen mainly because it uses the R_{jb} distance that takes into account rupture geometry instead of the epicentral. At the same time, disaggregation of the PP00 model is of less interest, as earthquakes with magnitudes $5.0 \leq \mathbf{M} \leq m_{max}$ have an equal probability to occur anywhere in the zone's surface.

In **Table 3** the most probable scenarios to cause PGA greater than the value that corresponds to a mean return period of 475 is presented. An interesting remark is that the scenario that has the biggest contribution is in the magnitude range of **M** [6.3-6.7] for all four sites. For Mytilene and Sigri the highest contribution is in the same distance range **R** (km) [20-30], while in shorter distance ranges for Mithymna and Vrisa.

Table 3 - PSHA calculations for the four sites of interest and a mean return period of 475 years.

Mean Return Period 475 years	**Distance, R (km)**	**Magnitude, M**	**SA (0.2 sec) (g)**
Mytilene	20 – 30	6.3 – 6.7	0.94
Vrisa	0 – 10	6.3 – 6.7	1.18
Mithymna	10 – 20	6.3 – 6.7	1.14
Sigri	20 - 30	6.3 – 6.7	0.93

In **Fig. 8** the hazard disaggregation is summarized for a mean return period of 475 years for the four examined sites. The two axes on the horizontal plane represent magnitude and distance ranges, while the vertical axis represents the relative contribution to seismic hazard, in terms of PGA, as a percentage of the final probability of exceedance (10% in 50 years). It can be observed that Vrisa and Mithymna, being close to the Agia Paraskevi and Edremit faults, respectively, show elevated values in small distance bins, compared to Sigri and Mytilene.

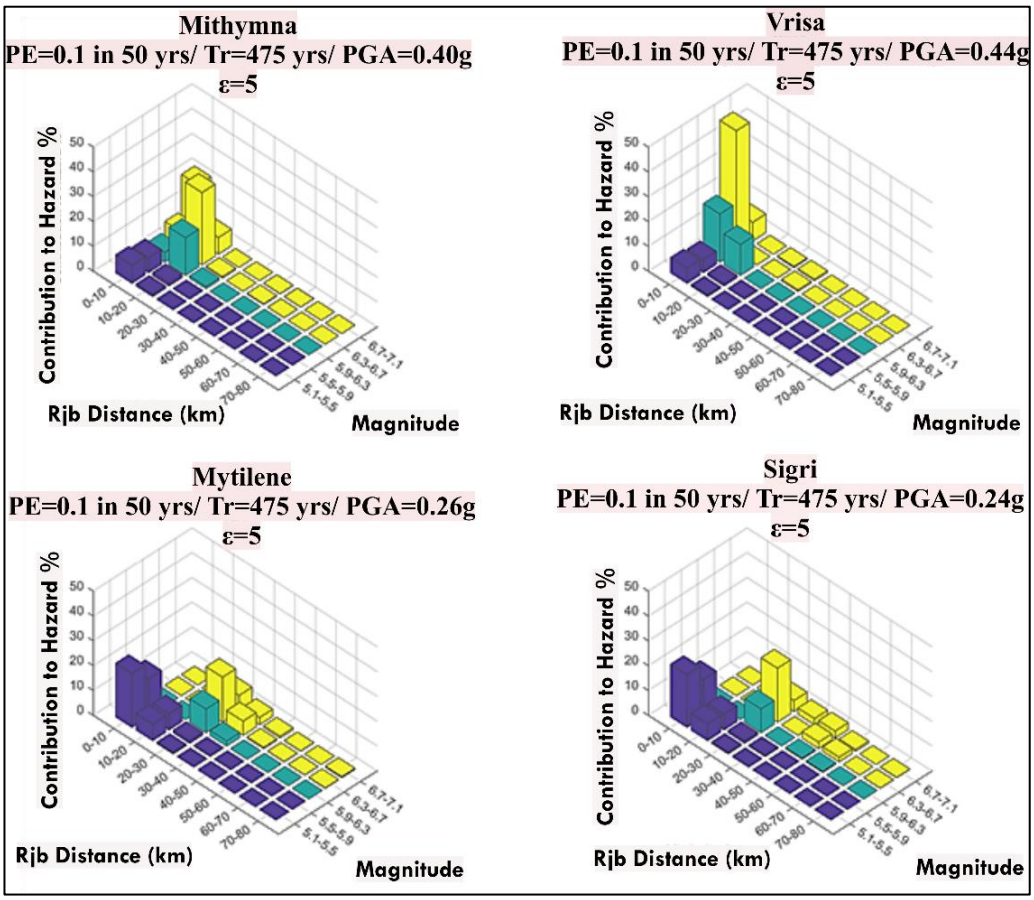

Fig. 8 Disaggregation charts depicting the relative contribution of different magnitude and distance ranges to the hazard. They refer to a mean return period of 475 years, the PPZ01 model, while using the GMPE of Akkar and Bommer (2010). A constant value of ε=5 was used. Note that for clarity a small percentage may be missing from the charts.

Finally, the percentage of exceedance probability for different values of (ε), for a total 0.1 probability of exceedance in 50 years can be seen in **Fig. 9**, for the four sites of interest. It can be observed that at least 50 % of the exceedance probability is between a^* and a_2 (where a^* is the value that corresponds to a 10% probability of exceedance in 50 years and a_2 the predicted value for ε=2), whereas at least 95% between a^* and a_3 (the predicted value for ε=3). This indicates that a truncation to a value higher than ε=3

would almost not affect the results at all for a 0.1 probability of exceedance in 50 years. This indicates that a truncation to a value higher than ε=3 would almost not affect the results at all for a 0.1 probability of exceedance in 50 years.

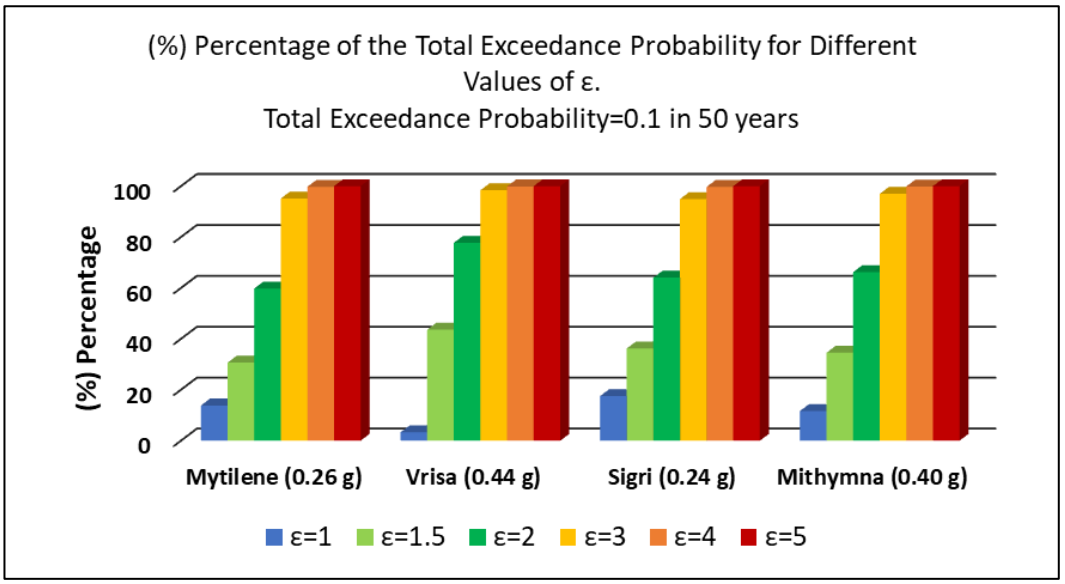

Fig. 9 Percentage of exceedance probability (Total Exceedance Probability= 0.1 in 50 years) for different values of (ε) (e.g. numbers of standard deviation from the median value) for the four sites of interest examined in this study. The PPZ01 seismic source model and the AK10 GMPE were used for the calculations.

4. CONCLUSIONS

We examined the seismic hazard of Lesvos Island, using the most updated modules of the R-CRISIS software, aiming to examine the variability captured by various appropriate GMPEs and seismic source models. The main conclusions can be summarized as:

- The calculated seismic hazard for selected sites on the island is in accordance with the predictions of existing EU hazard models.
- The calculations are found to be sensitive on weight choice in terms of both seismic sources (**Fig.** 6) and GMPEs (**Fig. 5**).
- Further investigation is required, which will incorporate recent available data into PSHA software like R-CRISIS. The effect of weighting factors among the logic tree branches and the different parameter choices (e.g. the minimum magnitude) also needs to be investigated in detail through sensitivity analysis. In addition, the

incorporation of local site effects, which significantly amplify the expected values, is an issue of further research.

- Almost the entire probability of exceedance, using a lognormal distribution for the GMPE's probability density function is between a* and a_3 (where a* is the value that corresponds to a 10% probability of exceedance in 50 years and a_3 the predicted value for ε=3). This is an observation made using only the Akkar and Bommer (2010) GMPE due to software limitations. Further investigation is needed in order to draw a general conclusion.
- We must note that significant uncertainties arise from poorly mapped off-shore faults and their unknown recurrence times, or known active faults for which the data is not yet sufficient to include them into PSHA calculations.
- Finally, the performance of the available GMPEs for the broader Aegean Sea region is another issue for further investigation. To date the available choices in terms of spectral values are very limited.

5. ACKNOWLEDGEMENTS

We acknowledge support of this work by the project "HELPOS – Hellenic System for Lithosphere Monitoring" (MIS 5002697) which is implemented under the Action "Reinforcement of the Research and Innovation Infrastructure", funded by the Operational Programme "Competitiveness, Entrepreneurship and Innovation" (NSRF 2014-2020) and co-financed by Greece and the European Union (European Regional Development Fund). We thank the editor and two anonymous reviewers for their constructive comments that led to substantial improvement of this manuscript.

6. REFERENCES

Abrahamson, N. A., 2006. Seismic Hazard Assessment: Problems with Current Practice and Future Developments. *Proceedings, First European Conference on Earthquake Engineering and Seismology, Geneva, Switzerland*.

Abrahamson N. A., Silva W.J., Kamai R., 2014. Summary of the ASK14 Ground Motion Relation for Active Crustal Regions. *Earthquake Spectra*. 30:1025-1055.

Akkar, S., Bommer J.J., 2010. Empirical equations for the prediction of PGA, PGV and spectral accelerations in Europe, the Mediterranean region and the Middle East. *Seismological Research Letters*, 81, 195-206.

Basili, R., Kastelic, V., Demircioglu, M. B., Garcia Moreno, D., Nemser, E. S., Petricca, P., Sboras, S. Besana-Ostman, G., Cabral, J., Camelbeeck, T., Caputo, R., Danciu, L., Domac, H., Fonseca, J., García-Mayordomo, J., Giardini, D., Glavatovic, B., Gulen, L., Ince, Y., Pavlides, S., Sesetyan, K., Tarabusi, G., Tiberti, M., Utkucu, M., Valensise, G., Vanneste, K., Vilanova, S., Wössner, J., 2013. The European Database of Seismogenic Faults (EDSF) *compiled in the framework of the Project SHARE*. http://diss.rm.ingv.it/share-edsf/, doi: 10.6092/INGV.IT-SHARE-EDSF13.

Bazzurro, P., Cornell, C.A., 1999. Disaggregation of seismic hazard, *Bull. Seismol. Soc. Am.*, 89(2), 501–520.

Bommer, J., Crowley H., 2017. The Purpose and Definition of the Minimum Magnitude Limit in PSHA Calculations. *Seismological Research Letters*, 88, 1097–1106.

Bommer, J., Scherbaum F., 2008. The Use and Misuse of Logic Trees in Probabilistic Seismic Hazard Analysis. *Earthquake Spectra*, 24, 997-1009.

Bommer, J., Scherbaum, F., Bungum, H., Cotton, F., Sabetta, F., Abrahamson, N., 2005. On the Use of Logic Trees for Ground-Motion Prediction Equations in Seismic-Hazard Analysis. *Bulletin of the Seismological Society of America*, 95, 377-389.

Bommer, J., Stafford, P.J., Alarcon, J.E., Akkar, S., 2007. The influence of magnitude range on empirical ground motion. *Bulletin Seismological Society of America*, 97, 2152–2170.

Boore D.M., Stewart J.O., Seyhan E., Atkinson G.M., 2014. NGA-West2 Equations for Predicting PGA, PGV, and 5% Damped PSA for Shallow Crustal Earthquakes. *Earthquake Spectra*, 30, 1057-1085.

Budnitz, R., Apostolakis, G., Boore, D., Cluff, L., Coppersmith, K., Cornell, C., Morris, P., (1997). Recommendations for Probabilistic Seismic Hazard Analysis: Guidance on Uncertainty and Use of Experts: Main Report (NUREG/CR-6372, Volume 1), available at https://www.nrc.gov/docs/ML0800/ML080090003.pdf .

Campbell, K., & Bozorgnia, Y., (2014). NGA-West2 ground motion model for the average horizontal components of PGA, PGV, and 5% damped linear acceleration response spectra. *Earthquake Spectra*, 30, 1087-1115.

Chatzipetros, A., Kiratzi, A., Sboras, S., Zouros, N., Pavlides, S., 2013. Active faulting in the north-eastern Aegean Sea Islands. *Tectonophysics*, 597-598, pp. 106-122.

Chiou B., Youngs R., 2014. Update of the Chiou and Youngs NGA Model for the Average Horizontal Component of Peak Ground Motion and Response Spectra. *Earthquake Spectra*, 30, 1117-1153.

Chousianitis, K., Del Gaudio, V., Pierri, P., Tselentis, G., 2018. Regional ground-motion prediction equations for amplitude-, frequency response-, and duration-based parameters for Greece. *Earthquake Engineering & Structural Dynamics*, 47, 2252-2274.

Cornell, C.A., 1968. Engineering seismic risk analysis. *Bull. Seism. Soc. Am.*, 58, 1503-1606.

Cornell, C. A., 1971. Probabilistic analysis of damage to structures under seismic loads, in: D.A. Howells, I.P. Haigh and C. Taylor. (Eds.), *Dynamic Waves in Civil Engineering: Proceedings of a Conference Organized by the Society for Earthquake and Civil Engineering Dynamics.* John Wiley, New York, 473-493 pp.,

Cotton, F., Scherbaum, F., Bommer, J.J., Bungam, H., 2006. Criteria for selecting and adjusting ground –motion models for specific target regions: application to Central Europe and rock sites. *Journal of Seismology*, 10, 137–156.

Danciu, L., Tselentis G-A., 2007. Engineering ground-motion parameters attenuation relationships for Greece. *Bulletin Seismological Society of Americ*a, 97, 162-183.

EAK, 2003. Greek Seismic Code. Earthquake Planning & Protection Organization. Athens-Greece, ed., 72 pp and 7 appendixes (in Greek).

EPRI (2006). Program on Technology Innovation: Truncation of the lognormal distribution and value of the standard deviation for ground motion models in the Central and eastern United States, EPRI, Palo Alto, CA and the U.S. Department of Energy: 2006, Report #1013105.

Esteva, L., 1970. Seismic risk and seismic design descriptions, in: R. J. Hansen (Eds.), *Seismic Design for Nuclear Power Plants*. MIT Press, 142-182.

Giardini D. et al., 2013. Seismic Hazard Harmonization in Europe (SHARE): Online Data Resource, doi: 10.12686/SED-00000001-SHARE, 2013.

Giardini, D., Woessner J., Danciu L., 2014. Mapping Europe's Seismic Hazard. *EOS*, 95, 261-262.

Hatzidimitriou, P. M., Papazachos B. C., and G. F. Karakaisis., 1994. Quantitative seismicity of the Aegean and surrounding area, *Proc. Of the XX1V Gen. Assembly of E.S.C., Athens, 19-24 September 1994*, 155-164.

Joyner, B., Boore, D., 1981. Peak horizontal acceleration and velocity from strong-motion records including records from the 1979 Imperial Valley, California, earthquake. *Bulletin of the Seismological Society of America*, 71, 2011–2038.

Kahle, H.G., Straub, C., Reilinger, R., McClusky, S., King, R., Hurst, K., Veis, G., Kastens, K., Cross, P., 1998. The strain rate field in the eastern Mediterranean region estimated by repeated GPS measurements. *Tectonophysics*, 294, 237–252.

Kiratzi, A., 2018. The 12 June 2017 Mw 6.3 Lesvos Island (Aegean Sea) earthquake: Slip model and directivity estimated with finite-fault inversion. *Tectonophysics*, 724-725, 1-10.

Kiratzi, A., Karakaisis, G., Papadimitriou, E., Papazachos, B., 1985. Seismic source-parameter relations for earthquakes in Greece. *Pure and Applied Geophysics*, 123, 27-41.

Kulkarni, R. B., Youngs R. R., Coppersmith K. J., 1984. Assessment of confidence intervals for results of seismic hazard analysis. *Proceedings of the Eighth World Conference on Earthquake Engineering, San Francisco*, 263–270.

Makropoulos, K. C., Burton P., 1985. Seismic hazard in Greece. II. Ground acceleration. *Tectonophysics*, 117, 259-294.

Margaris, B., Papazachos, C., Papaioannou, C., Theodulidis, N., Kalogeras, I. S., Skarlatoudis, A., 2002. Ground motion attenuation relations for shallow earthquakes in Greece, *Proc. Of Twelfth European Conference on Earthquake Engineering*, 318–327.

Mavroulis, S., Andreadakis, E., Spyrou, N.-I., Antoniou, V., Skourtsos, E., Papadimitriou, P., Kassaras, I., Kaviris, G., Tselentis, G.-A., Voulgaris, N., Carydis, P., Lekkas, E., 2019. UAV and GIS based rapid earthquake-induced building damage assessment and application of the EMS-98 for the June 12, 2017 Mw 6.3 Lesvos (Northeastern Aegean, Greece). *Int. J. Disaster Risk Reduction*, 37, 101169.

McGuire, R., 1995. Probabilistic seismic hazard analysis and design earthquakes: closing the loop. *International Journal of Rock Mechanics and Mining Sciences & Geomechanics Abstracts*, 33, A294.

McGuire, R. K., 2004. Seismic Hazard and Risk Analysis. Oakland, CA: Earthquake Engineering Research Institute, 240 pp.

Moratto, L., Orlecka – Sikora, B., Costa, G., Suhadolc, P., Papaioannou, Ch., Papazachos C. B., 2007. A deterministic seismic hazard analysis for shallow earthquakes in Greece. *Tectonophysics*, 442, 66 – 82.

Ordaz M., Reyes C., 1999. Earthquake hazard in Mexico City: Observations versus computations. *Bulletin of the Seismological Society of America*, 89, 1379–1383.

Ordaz, M., Martinelli, F., Aguilar, A., Arboleda, J., Meletti, C., D' Amico, V., 2017. R-CRISIS. Program and platform for computing seismic hazard, available at http://www.r-crisis.com/about/crisis/.

Ordaz, M., Salgado-Gálvez, M.A., 2017. R-CRISIS Validation and Verification Document. Technical Report. Mexico City, Mexico; available at [http://www.r-crisis.com/knowledge/documentation/].

Papadimitriou, P., Kassaras, I., Kaviris, G., Tselentis, G.A., Voulgaris, N., Lekkas, E., Chouliaras, G., Evangelidis, C., Pavlou, K., Kapetanidis, V., Karakonstantis, A., Kazantzidou-Firtinidou, D., Fountoulakis, I., Millas, C., Spingos, I., Aspiotis, T., Moumoulidou, A., Skourtsos, E., Antoniou, V., Andreadakis, E., Mavroulis, S., Kleanthi, M., 2018. The 12th June 2017 Mw = 6.3 Lesvos earthquake from detailed seismological observations, *J. Geodyn.*, 115, 23–42.

Papaioannou, Ch. A., Papazachos, B.C., 2000. Time-independent and time-dependent seismic hazard in Greece based on seismogenic sources, *Bulletin of the Seismological Society of America*, 90, 22-33.

Papazachos, B.C., Kiratzi, A.A. and Karakostas, B.G., 1997. Toward a homogeneous moment-magnitude determination for earthquakes in Greece and surrounding area, *Bull. Seism. Soc. Am.* 87, 474–483.

Papazachos, B. C., Papazachou C., 2003. The Earthquakes of Greece. Ziti Publ., Thessaloniki.

Papazachos, B.C., Mountrakis, D.M., Papazachos, C.B., Tranos, M.D., Karakaisis, G.F., Savvaidis, A.S., 2001. The faults that caused the known strong earthquakes in Greece and surrounding areas during 5th century B.C. up to present, *Proc. 2nd Conf. Earthquake Eng. and Eng. Seism., 2-30 September 2001, Thessaloniki, Greece*, 1, 17-26.

Papazachos, B. C., Scordilis, E., Panagiotopoulos, D., Papazachos, C., Karakaisis, G., 2004. Global Relations Between Seismic Fault Parameters and Moment Magnitude of Earthquakes. *Bulletin of the Geological Society of Greece*, XXXVI, 1482-1489.

Reilinger, R., McClusky, S.C., Oral, M.B., King, R.W., Toksoz, M.N., Barka, A.A., Kinik, I., Lenk, O., Sanli, I., 1997. Global positioning system measurements of present-day crustal movements in the Arabia-Africa-Eurasia plate collision zone. *J. Geophys. Res.*, 102, 9983–9999.

Reiter, L., 1990. Earthquake Hazard Analysis: Issues and Insights. Columbia University Press, New York.

SEAHELLARC Working Group, 2010. Preliminary seismic hazard assessments for the area of Pylos and surrounding region (SW Peloponnese). *Bollettino di Geofisica Teorica ed Applicata*, 51, 163-186.

Segou, M., Voulgaris, N. 2013. The Use of Stochastic Optimization in Ground Motion Prediction. *Earthquake Spectra*, 29, 283-308.

Skarlatoudis, A., Papazachos, C., Margaris, B., Theodulidis, N., Papaioannou, C., Kalogeras, I., Scordilis, E., Karakostas, V., 2003. Empirical Peak Ground-Motion Predictive Relations for Shallow Earthquakes in Greece. *Bulletin of the Seismological Society of America*, 93, 2591-2603.

Skarlatoudis, A., Papazachos, C., Margaris, B., Theodulidis, N., Papaioannou, C., Kalogeras, I., Scordilis, E., Karakostas, V., 2007. Erratum to Empirical Peak Ground-Motion Predictive Relations for Shallow Earthquakes in Greece. *Bulletin of the Seismological Society of America*, 97, 2219-2221.

Stylianou E., Maravas, G., Kouskouna V., Papoulia J., 2016. Seismic hazard assessment in the North Aegean Trough based on a new seismogenic zonation. *Bulletin of the Geological Society of Greece*, 50 (3), 1443-1452.

Taymaz, T., Jackson, J.A., McKenzie, D., 1991. Active tectonics of the North and Central Aegean Sea. *Geophys. J. Int*., 106, 433–490.

Theodulidis, N. P., 1991. Contribution to strong ground motion study in Greece. Ph.D. Thesis, Aristotle University of Thessaloniki, Thessaloniki, 500 p.

Theodulidis, N. P., Papazachos B. C., 1992. Dependence of strong ground motion on magnitude-distance, site, geology and macroseismic intensity for shallow earthquakes in Greece: I, peak horizontal acceleration, velocity and displacement. *Soil Dynamics and Earthquake Engineering*, 11, 387-402.

Thomas, P., Wong, I., Abrahamson, N., 2010. Verification of probabilistic seismic hazard analysis computer programs. *Pacific Earthquake Engineering Research Center. PEER 2010/106 Report.* California, USA.

Tselentis, G., Danciu, L., 2010. Probabilistic seismic hazard assessment in Greece – Part 1: Engineering ground motion parameters. *Natural Hazards and Earth System Science*, 10, 25-39.

Vamvakaris, D., Papazachos, C., Papaioannou, C., Scordilis, E., Karakaisis, G., 2016. Seismic Hazard Assessment in The Broader Aegean Area Using Time-Independent Seismicity Models Based on Synthetic Earthquake Catalogues. *Bulletin of the Geological Society of Greece*, 50, 1463-1472.

Weatherill, G., Burton, P., 2010. An alternative approach to probabilistic seismic hazard analysis in the Aegean region using Monte Carlo simulation, *Tectonophysics*, 492, 253-278.

Woessner, J., Danciu L., D. Giardini and the SHARE consortium, 2015. The 2013 European Seismic Hazard Model: key components and results, *Bull. Earthq. Eng*., doi:10.1007/s10518-015-9795-1.